The International Journal of Robotics Research

http://ijr.sagepub.com/

The Devon Island rover navigation dataset

Paul Furgale, Pat Carle, John Enright and Timothy D Barfoot

The International Journal of Robotics Research 2012 31: 707 originally published online 16 April 2012
DOI: 10.1177/0278364911433135

The International Journal of
Robotics Research
31(6) 707–713

DOI: 10.1177/0278364911433135
ijr.sagepub.com

The Devon Island rover navigation dataset

Paul Furgale[1]*, Pat Carle[2], John Enright[3] and Timothy D Barfoot[2]

Abstract

In this paper we present a rover navigation dataset collected at a Mars/Moon analogue site on Devon Island, in the Canadian High Arctic. The dataset is split into two parts. The first part contains rover traverse data: stereo imagery, Sun vectors, inclinometer data, and ground-truth position information from a differential global positioning system (DGPS) collected over a 10-km traverse. The second part contains long-range localization data: 3D laser range scans, image panoramas, digital elevation models, and GPS data useful for global position estimation. All images are available in common formats and other data is presented in human-readable text files. To facilitate use of the data, Matlab parsing scripts are included.

Keywords

stereo vision, visual odometry, global localization, lidar, digital elevation model

1. Introduction

In this paper we describe a large dataset collected at a Moon/Mars analogue site on Devon Island in the Canadian High Arctic. Devon Island presents unique qualities for planetary analogue studies because it offers an unusually wide variety of geological features and microbiological attributes of strong planetary analogue value or potential (Lee et al. 2007). It has been used for rover testing in the past (Barfoot et al. 2010), because it presents real challenges to field exploration that are analogous in fundamental ways to those expected in planetary exploration. Being an impact basin in a polar desert environment, the lack of vegetation and variety of terrain make it well suited for rover field tests.

The dataset presented here is suitable for researchers interested in localization in global positioning system GPS-denied environments. The dataset is partitioned into two parts: (1) rover traverse data including stereo images, Sun vectors, inclinometer data, and differential global positioning system (DGPS) position, and (2) long-range localization data including long-range lidar scans, image panoramas, digital elevation models, and GPS position. The full dataset is available at

http://asrl.utias.utoronto.ca/datasets/devon-island-rover-navigation

This web page also includes extensive descriptions of all available data and file formats.

The rest of this paper is organized as follows. Section 2 introduces the rover traverse data, including frame conventions and calibration values. Section 3 describes the long-range localization data.

2. Rover traverse data

Stereo imagery, Sun vectors, inclinometer data, and DGPS were collected using an unactuated pushcart outfitted with typical rover engineering sensors. The rover platform traveled 10 km, starting at 10:00 near the Haughton-Mars Project Research Station (Lee et al. 2007) and returning in a large loop to the start by 18:00 (Figure 1).

The traverse passes through many areas exhibiting the unique, vegetation-free, planetary-analogue terrain that Devon Island is known for: rocky canyons, boulder fields,

[1]Eidgenössische Technische Hochschule Zürich, Switzerland
[2]University of Toronto Institute for Aerospace Studies, Toronto, ON, Canada
[3]Department of Aerospace Engineering, Ryerson University, Toronto, ON, Canada

*The work described in this paper was conducted while at the University of Toronto Institute for Aerospace Studies.

Corresponding author:
Paul Furgale, Eidgenössische Technische Hochschule Zürich, Tannenstrasse 3, 8092 Zürich, Switzerland
Email: paul.furgale@mavt.ethz.ch

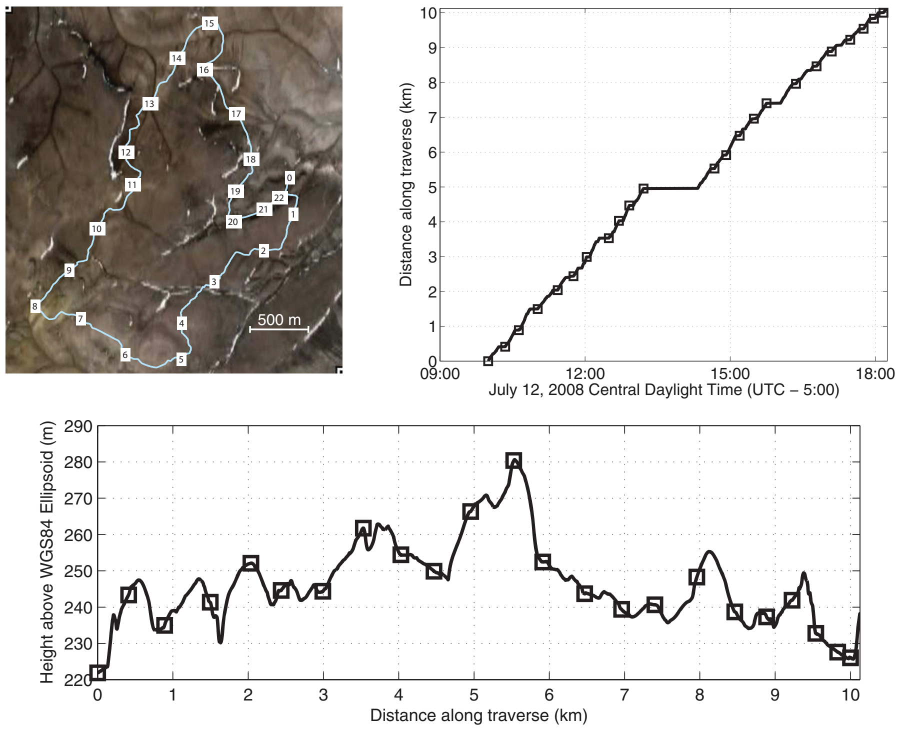

Fig. 1. Plots of the rover traverse: (top left, image credit: Google Earth, © 2011 Google, © 2011 DigitalGlobe) a map of the rover traverse showing the start of each subsequence; (top right) a plot of distance traveled versus time of day; and (bottom) the elevation change over the course of the traverse. The platform orientation at the start of each subsequence has been estimated using a batch of Sun vectors and inclinometer readings to allow easy comparison with the GPS track.

sandy flats, and significant topographic relief. When collecting the data, every effort was made to ensure that a minimum of man-made objects were in view of the camera. The resulting images, coupled with data from the other sensors and excellent ground-truth position information, make a truly unique dataset relevant both to the mobile robotics and planetary exploration researchers.

For ground-truth position, a pair of Magellan ProMark3 GPS units were used to produce post-processed DGPS data for the whole traverse. The rover traverse is partitioned into 23 sections. At the start of each section, a batch of Sun vectors and inclinometer readings was collected and the method described by Furgale et al. (2011) was used to estimate the rotation between the Sun sensor frame and the topocentric frame. These known orientations provide a convenient way to compare motion estimates to the GPS data.

A single computer logged timestamped stereo images, inclinometer readings, and Sun sensor data. The images in the dataset were collected using an odometric trigger with approximately one image collected every 20 cm traveled. The Sun sensor and inclinometer each produced data at approximately 1 Hz, but logging was paused when the cart was stationary. The DGPS was logged at 1 Hz on a pair of independent Magellan ProMark3 GPS units. At the start of the day, the logging computer's clock was synchronized with a National Institute of Standards and Technology (NIST) time server using the Network Time Protocol (NTP). The computer time over the course of the day should be accurate to approximately 1 second.

This data is suitable for research into position and orientation estimation such as visual odometry or celestial navigation. Full-resolution color imagery is provided for the entire traverse, allowing researchers to evaluate changes in algorithm in performance as image resolution is reduced or color information is ignored.

The cart and relevant coordinate frames are shown in Figure 2 and described in Table 1. We use an axis-angle representation of rotations. Given a unit vector axis, $\mathbf{a}$, and an angle, r, a rotation matrix, $\mathbf{C}$, may be built using

$$\mathbf{C}(\mathbf{a}, r) := \mathbf{a}\mathbf{a}^T + \left(\mathbf{1} - \mathbf{a}\mathbf{a}^T\right)\cos(r) - \mathbf{a}^\times \sin(r), \quad (1)$$

where $(\cdot)^\times$ is the skew-symmetric matrix operator that can be used to implement the cross product,

$$\begin{bmatrix} x \\ y \\ z \end{bmatrix}^\times := \begin{bmatrix} 0 & -z & y \\ z & 0 & -x \\ -y & x & 0 \end{bmatrix}. \quad (2)$$

To express translations, we use the notation $\boldsymbol{\rho}_a^{ba}$ to mean the vector from the origin of $\underrightarrow{\mathcal{F}}_a$ to the origin of $\underrightarrow{\mathcal{F}}_b$ (denoted by the superscript), expressed in $\underrightarrow{\mathcal{F}}_a$ (denoted by the subscript). Using this notation, we may build a 4×4

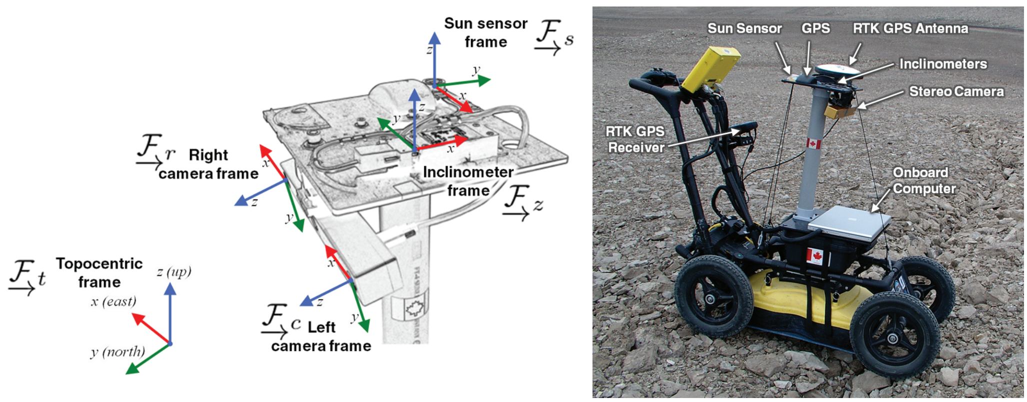

Fig. 2. The platform used to collect the rover navigation data.

Table 1. Reference frames relevant to the rover traverse data.

Coordinate Frame	x-axis	y-axis	z-axis
$\underrightarrow{\mathcal{F}}_t$ topocentric	East	North	Up
$\underrightarrow{\mathcal{F}}_c$ left camera	Horizontal pixels	Vertical pixels	Optical axis
$\underrightarrow{\mathcal{F}}_r$ right camera	Horizontal pixels	Vertical pixels	Optical axis
$\underrightarrow{\mathcal{F}}_s$ sun sensor	Toward connector		Optical axis
$\underrightarrow{\mathcal{F}}_z$ inclinometer	Away from connector		Up
$\underrightarrow{\mathcal{F}}_g$ GPS antenna	—	—	—

Table 2. Parameters for the relative coordinate frame transformations between sensors. See Table 1 for the coordinate frame definitions. A transformation, $\boldsymbol{T}_{ab}$, may be constructed using (3) from a row of this table by building $\boldsymbol{\rho}_a^{ba} = [x\ y\ z]^T$, $\mathbf{a}_{ab} = [a_1\ a_2\ a_3]^T$, and $\mathbf{C}_{ab} = \mathbf{C}(\mathbf{a}_{ab}, r)$ from (1).

Transformation	x (m)	y (m)	z (m)	a_1	a_2	a_3	r (rad)
$\boldsymbol{T}_{sz}$	0.18	−0.09	0.00	−0.013	−0.005	−0.999	1.56
$\boldsymbol{T}_{sc}$	0.21	−0.17	−0.09	−0.015	−0.790	0.612	−3.11
$\boldsymbol{T}_{cr}$	0.24	0.00	0.00	1.000	0.000	0.000	0.00
$\boldsymbol{\rho}_s^{gs}$	0.20	−0.12	0.03	—	—	—	—

transformation matrix, $\boldsymbol{T}_{ab}$, that takes points from $\underrightarrow{\mathcal{F}}_b$ to $\underrightarrow{\mathcal{F}}_a$ as

$$\boldsymbol{T}_{ab} := \begin{bmatrix} \mathbf{C}_{ab} & \boldsymbol{\rho}_a^{ba} \\ \mathbf{0}^T & 1 \end{bmatrix}, \tag{3}$$

where $\mathbf{0}$ is the zero matrix.

The parameters for the inter-sensor transformation matrices are given in Table 2. The inter-sensor rotations were obtained using the calibration method described by Furgale et al. (2011) and have an uncertainty of the order of 1° (one sigma). The translations between sensors were hand measured with an uncertainty of a few centimeters.

2.1. Data formats

Table 3 provides an overview of the data collected and Table 4 summarizes the file formats. To further simplify previewing the data, color videos of the stereo images (with frame numbers embedded) are available for download. Complete details of the data formats are available on the dataset website.

3. Long-range localization data

Lidar scans and panoramic images were acquired at 37 different locations on Devon Island with the Optech ILRIS3D-ER[1] shown in Figure 3. The point clouds from

Fig. 3. Top: an Optech ILRIS3D-ER mounted on a motorized pan–tilt unit was used to collect 37 long-range lidar scans. Bottom: an image panorama collected with the scan.

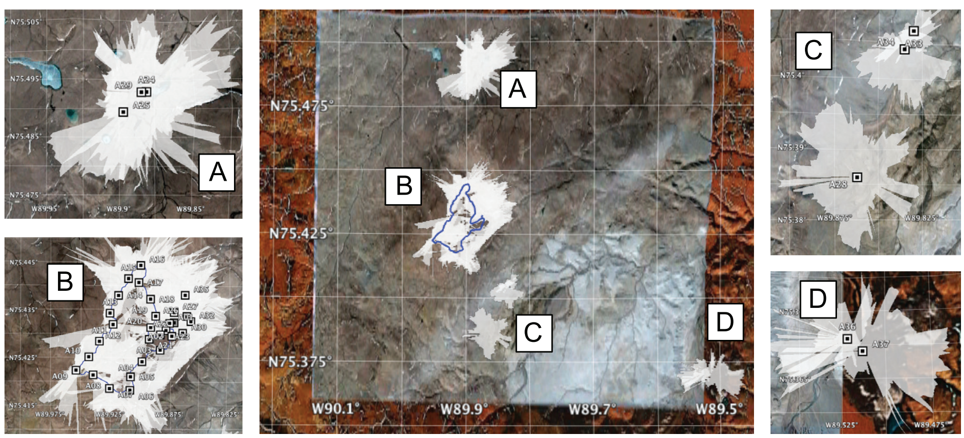

Fig. 4. Plots showing the coverage of the lidar scans (Image credit: Google Earth, © 2011 Google, © 2011 DigitalGlobe, © 2011 TerraMetrics). Light-shaded areas have been imaged by the lidar. The solid (blue) line in the central figure and in (B) is the path of the rover from Section 2. This preview is available on the dataset website as a kmz file compatible with Google Earth.

Table 3. An overview of the data logged during the rover traverse.

Sensor	Description	Data logged	Measurements	Capture rate
Camera	Point Grey Research Bumblebee XB3 24 cm baseline stereo camera	Color 1,280 × 960 images	49,410 pairs	Approximately one image every 20 cm
Sun sensor	Sinclair Interplanetary SS-411 digital Sun sensor	Sun zenith and azimuth	15,256	1 Hz
Inclinometer	Honeywell HMR-3000 inclinometer	Pitch and roll	17,257	1 Hz
DGPS	A pair of Magellan ProMark3 GPS units	Latitude, longitude, and elevation expressed with respect to the WGS84 ellipsoid	30,734	1 Hz

these 360° scans contain millions of points spread out over a maximum range of about 1.5 km with centimeter-scale position accuracy. A camera on the lidar also allowed panoramic images to be collected. Before each scan, the lidar was leveled with a two-axis bubble level to an accuracy of about 1° (one sigma). To obtain the heading of the

Table 4. An overview of the log files available for the rover traverse. Images are provided as .ppm (color) or .pgm (monochrome) files. All other data files are provided as space-separated ASCII.

File	Description	Format
color-raw-1280x960-{left,right}-[index].ppm	Color, 1,280 × 960, raw stereo image pairs	.ppm
color-rectified-1280x960-{left,right}-[index].ppm	Color, 1,280 × 960, rectified stereo image pairs	.ppm
grey-rectified-512x384-{left,right}-[index].pgm	Monochrome, 512 × 384, rectified stereo image pairs	.pgm
lut-{left,right}-{x,y}.txt	Rectification look up tables for the 1,280 × 960 left and right images	1,280 × 960 matrix
image-times.txt	Image timestamps	Image index, timestamp
known-orientations.txt	Rover attitude estimates at subsequent start locations	Image index, rotation parameters for $\mathbf{C}_{tc}$
inclinometer.txt	Inclinometer readings	Timestamp, pitch (degrees), roll (degrees)
inclinometer-sampled.txt	Inclinometer readings sampled at the image times	image index, pitch (degrees), roll (degrees), timestamp offset (s)
sun-sensor.txt	Sun sensor readings	Timestamp, azimuth (degrees), zenith (degrees)
sun-sensor-sampled.txt	Sun sensor readings sampled at the image times	Image index, azimuth (degrees), zenith (degrees), timestamp offset (s)
gps-latlngele.txt	DGPS expressed with respect to the WGS84 ellipsoid	Timestamp, latitude (degrees), longitude (degrees), elevation (m)
gps-latlngele-sampled.txt	DGPS sampled at the image times	Image index, latitude (degrees), longitude (degrees), elevation (m)
gps-topocentric.txt	Metric displacement of the camera frame from the initial position (i.e. the position of the first image is $[0 \quad 0 \quad 0]^T$)	Image index, easting (m), northing (m), elevation (m)
gps-utm.txt	DGPS in UTM coordinates	Timestamp, easting (m), northing (m), elevation.

lidar with respect to the Easting, a target was setup about 100 m away and scanned. Using the position of the lidar and the position of the target from GPS, we determined the heading of the lidar to approximately 1° (one sigma). See Carle et al. (2010) for further details. Figure 4 depicts an overview of the lidar scan coverage, and shows the relationship of the lidar scans to the rover traverse from Section 2. This visualization of the dataset is available as a kmz file compatible with Google Earth.[2]

Orbital maps, or Digital Elevation Models (DEMs), of Devon Island were obtained from Geobase[3] on 11 December 2009. The maps were projected from North American Datum 1983 (NAD83) latitude/longitude coordinates to the Universal Transverse Mercator (UTM) coordinate system using the commercial program Global Mapper.[4] The elevation data in the maps is expressed in the Canadian Geodetic Vertical Datum 1928 (CGVD28). The UTM maps may be easily compared with the raw

Table 5. An overview of the long-range localization data available.

Sensor	Description	Data available	Measurements
Lidar	Optech ILRIS3D-ER	Long-range 360° lidar scans with 3D points, intensity	37
Camera	Optech ILRIS3D-ER integrated camera	360° panoramic images	37
GPS	Garmin GPSMAP 76CSx	UTM position	37
—	Digital Elevation Models	UTM position, CGVD28 elevation	Two maps covering all scan locations

Table 6. An overview of the log files available for the long range localization data. Images are provided as .png. All other data files are provided as space-separated ASCII.

File	Description	Format
A[index].txt	360° panoramic lidar data	x (m), y (m), z (m), intensity
A[index].png	360° panoramic image	.png
groundtruth.txt	UTM position	UTM easting (m), UTM northing (m)
mapHiRes.txt	UTM position and CGVD28 elevation digital elevation model	UTM easting (m), UTM northing (m), elevation (m)
mapLoRes.txt	UTM position and CGVD28 elevation digital elevation model	UTM easting (m), UTM northing (m), elevation (m)

three-dimensional point data acquired by the lidar. Two maps are provided:

1. A 1:50,000 high-resolution map with each pixel covering an area approximately 13 m × 24 m. This was derived from Geobase maps '058h06' and '058h07'. Both of these maps were published in 2004. Geobase does not provide information about when the data were collected.
2. A 1:250,000 low-resolution map with each pixel covering an area approximately 50 m × 94 m. This was derived from Geobase map '058h'. This map was published in 1998. Geobase does not provide information about when the data were collected.

Ground-truth positions of the lidar scan locations were obtained from a Garmin GPSMAP 76CSx. After averaging GPS measurements for several minutes at each scan location, the standard deviation of position measurements was estimated to be 1 m.

The data is suitable for research into global position estimation. Data collected on the ground by the lidar (3D points, panoramic imagery) may be compared with the georeferenced DEMs to estimate the position of the lidar when the scan was taken.

3.1. Data formats

Table 5 provides an overview of the data available and Table 6 summarizes the file formats. Complete details of the file formats are available on the dataset website.

Notes

1. See http://www.optech.ca/i3dprodline-ilris3d.htm
2. Available at: http://asrl.utias.utoronto.ca/datasets/devon-island-rover-navigation/figs/devon-island-rover-navigation.kmz
3. Geobase (see http://www.geobase.ca/) is a repository of up-to-date geospatial data for Canadian territory maintained by the Canadian Council on Geomatics.
4. See http://www.globalmapper.com/

Funding

Funding for our field trials on Devon Island was provided by The Canadian Space Agency's Canadian Analogue Research Network (CARN) program (grant number CARN-08-01). The Natural Sciences and Engineering Research Council of Canada (NSERC) funded the remaining work.

Acknowledgements

The collection and processing of this data would not have been possible without the help of many people and we would like to thank some of them here. The Mars Institute and the Haughton-Mars Project provided infrastructure on Devon Island. Members of the communities of Resolute Bay, Grise Fjord, and Pond Inlet acted as guides, and protected us and our equipment from polar bears. Tom Lamarche from the Canadian Space Agency helped with our field testing. The authors would like to thank Mr Doug Sinclair of Sinclair Interplanetary for the donation of a SS-411 Digital Sun Sensor. Finally, at the University of Toronto Institute for Aerospace Studies, Konstantine Tsotsos and Peter Miras provided logistical support, and Rehman Merali pitched in during assembly of our pushcart rover.

References

Barfoot TD, Furgale PT, Stenning BE, Carle PJF, Enright JP and Lee P (2010) Devon island as a proving ground for planetary rovers. In *Proceedings of the Symposium on Brain, Body, and Machine,* a “Celebration of 25 Years of Research Excellence at the McGill Centre for Intelligent Machines”, Montreal, Quebec.

Carle P, Furgale PT and Barfoot TD (2010) Long-range rover localization by matching lidar scans to orbital elevation maps. *Journal of Field Robotics* 27: 344–370.

Furgale PT, Enright J and Barfoot TD (2011) Sun sensor navigation for planetary rovers: Theory and field testing. *IEEE Transactions on Aerospace and Electronic Systems* 47: 1631–1647.

Lee P, Braham S, Boucher M, Schutt J, Glass B, Gross A, et al. (2007) Haughton-Mars project: 10 years of science operations and exploration systems development at a moon/mars analog site on devon island, high arctic. In *Proceedings of the 38th Lunar and Planetary Science Conference*, League City, TX, pp. 2426–2427.